Bandwidth Improvement of Reflectarrays Using Single-Layered Double Concentric Circular Ring Elements

Lu Guo*, **Peng-Khiang Tan, and Tan-Huat Chio**

Abstract—In an effort to improve the bandwidth of the single layer reflectarray, this paper investigates the use of double concentric circular ring elements arranged in a range of sub-wavelength grids on a single layer of substrate. Compared to the traditional $\lambda/2$ grid arrangements, when the radiating elements are arranged in grids less than $\lambda/2$, the reflected phase is more uniform over a wider frequency bands when radiating elements' parameters are varied; albeit with a reduced reflected phase range. The double concentric circular ring elements used here also allow an additional degree-of-freedom to improve the bandwidth. A comprehensive investigation on reflectarrays' performance with various grid spacings is conducted and the trade-off between the reflectarray gain and bandwidth is also discussed. Based on the concentric ring element, four offset-fed $0.43\,\mathrm{m} \times 0.43\,\mathrm{m}$ reflectarrays centered at $10\,\mathrm{GHz}$ with various element periodicities, namely $\lambda/2$, $\lambda/3$, $\lambda/4$ and $\lambda/5$ grids, are designed and developed. The measured results show that among the four reflectarrays, the one with $\lambda/4$ grid spacing achieves the broadest 2-dB gain bandwidth of 33% with an aperture efficiency of 36.2%.

1. INTRODUCTION

Compared to parabolic dishes, reflectarrays have advantages of low profile, low mass and ease of fabrication. However, one major drawback of reflectarrays is their narrowband performance [1–3]. Numerous techniques have been proposed to improve the bandwidth of reflectarrays, such as multilayer designs [4, 5], single-layer multi-resonant designs [6, 7] and aperture coupled designs [8, 9]. An alternative method for broadband design has been introduced by using sub-wavelength elements instead of the conventional $\lambda/2$ elements [10–12]. It is demonstrated that the reflectarrays designed with sub-wavelength elements achieve a significant improvement in gain bandwidth performance. Nevertheless, to the authors' best knowledge, all the sub-wavelength element designs in the literatures so far are based on either single-layer [10, 11] or double-layer [12] single patch geometries. No research has been done on sub-wavelength single-layer multi-resonant elements, such as in the form of double concentric circular rings. The ring elements for broadband reflectarray antennas have been studied in [13–15]. It is demonstrated that a reasonable bandwidth and an increased reflected phase range can be achieved using the ring elements. By deploying single-layer multi-resonant elements with sub-wavelength grid spacing, one could benefit from both the simple structure and improved bandwidth performance.

In this paper, the bandwidth improvement of reflectarrays using single-layered double concentric circular ring elements on various sub-wavelength grids is investigated. Numerical studies are carried out to understand the broadband mechanism of single-layer sub-wavelength multi-resonant elements. The compromise between the reflectarray gain and bandwidth is also addressed. Based on these studies, four offset-fed X-band reflectarrays with various element periodicities, namely $\lambda/2$ (15 mm), $\lambda/3$ (10 mm), $\lambda/4$ (7.5 mm) and $\lambda/5$ (6 mm) grids, are designed and developed using variable sized double concentric circular rings. The various reflectarrays designed have relatively good performance except for the $\lambda/5$ case where the aperture efficiency is low. The one designed with $\lambda/4$ grid spacing demonstrates a remarkable 18% increase in the 2-dB gain bandwidth compared to the one with $\lambda/2$ grid spacing.

2. ELEMENT DESIGN AND ANALYSIS

In this study, a multi-resonant element in the form of variable sized double concentric circular rings is used. This is similar to the one in [6] where a relatively small 81-element single-layered reflectarray is built. While [6] shows a good bandwidth performance, the performance in a large array is not reported. This work deploys the elements in a much larger array of 729, 1640, 2809 and 4623 elements in a $0.43\,\text{m} \times 0.43\,\text{m}$ aperture with $\lambda/2$, $\lambda/3$, $\lambda/4$ and $\lambda/5$ grid spacings, respectively.

Figure 1 depicts the basic configuration of the element design. The double concentric circular ring elements are printed on a Rogers 4003 substrate with thickness of 8 mil, dielectric constant of 3.55 and loss tangent of 0.0027, supported by a layer of 3 mm polycarbonate ($\varepsilon r = 2.8$) and backed by a conducting ground plane. The element geometry offers an increased span of phase variation compared to the single circular ring, while the polycarbonate layer provides the necessary thickness for a slow varying phase variation when the double ring dimensions are changed. This is essential to obtain wideband performance. Note that one could even propose the triple concentric circular ring geometry to further increase the reflected phase span. However, it would somewhat complicate the optimization process when applied in sub-wavelength grids, owing to increased variables. Furthermore, it will be shown later that a phase variation range of about 300° is sufficient for designing the reflectarrays with a reasonable bandwidth. Therefore, the double concentric circular ring element has a good balance between the required reflected phase range and the degrees-of-freedom to improve the performance. The design operates at X-band centred at 10 GHz and the unit cell is analyzed using the commercial full-wave electromagnetic software Ansoft HFSS. The reflectarray is assumed to be formed by identical elements arranged in square lattices. Reflected phase and magnitude characteristics with four grid spacings, i.e., $\lambda/2$, $\lambda/3$, $\lambda/4$ and $\lambda/5$ are investigated to understand the broadband mechanism of single-layer sub-wavelength double concentric circular ring elements. The reflection response curves can be obtained by considering an infinite array of identical elements with a plane wave incidence upon them. It is noted that the reflection characteristics are dependent on the incident angle of the plane wave. However, it has been shown that the normal incidence can present good approximations for incident angles up to about 40° [16].
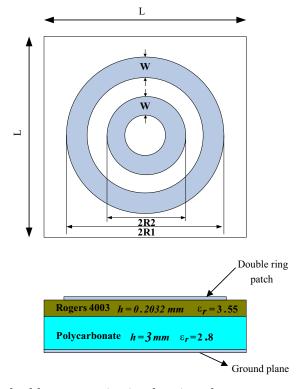

Figure 1. Geometry of the double concentric circular ring element.

2.1. The Effect of Double Concentric Circular Ring Spacing

It has been shown in the simulation that the linearity of the reflected phase curves is critically dependent on the double concentric circular ring spacing. Therefore the double ring spacing should be analyzed and optimized when applied on various grids. Fig. 2 plots the reflected phase curves with different double ring spacings at 10 GHz in a $\lambda/2$ grid while the ring width is fixed at $w = 0.08^*R1$. In Fig. 2, one notes that the double concentric ring spacing has a significant influence on the linearity of reflected phase curves. When the two rings are placed relatively further from each other, for example in the case of $R2 = 0.5R1$, $R2 = 0.6R1$ and $R2 = 0.7R1$, a "knee" is observed in the response curves. This is due to the two resonant frequencies which are related to the dimensions of two concentric double circular rings. When the two rings get closer, as in the cases of $R2 = 0.8R1$ and $R2 = 0.9R1$, the reflected phase curves become more linear and the range increases. One is able to obtain a span of phase change in excess of $600°$. Note that the $R2 = 0.8R1$ curve has a slightly smaller reflected phase range than the $R2 = 0.9R1$ curve, but the slope of the phase variation is less steep and therefore would result in a relatively broader bandwidth.
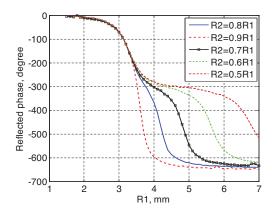

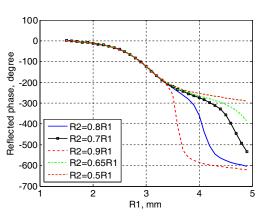**Figure 2.** Reflected phase curves with different ring spacings at 10 GHz in a $\lambda/2$ grid.

Figure 3. Reflected phase curves with different ring spacings at 10 GHz in a $\lambda/3$ grid.

Figure 3 is the same as Fig. 2 except that the grid spacing is $L = 10$ mm ($\lambda/3$). It is observed in Fig. 3 that the spacing between the two rings also affects the linearity of the phase curves quite significantly. However, a key difference is that increasing the ring spacing in a $\lambda/3$ grid leads to a more linear behaviour although the phase range is reduced. This is opposite of what is observed in the case of $\lambda/2$ grid. It is found that the curve of $R2 = 0.5R1$ shows a good linearity while offering a phase range about $300°$.

Figure 4 depicts the reflected phase curves with different ring spacings at 10 GHz in a $\lambda/4$ grid. It is interesting to observe that the linearity of the reflected phase curves is less sensitive to the ring spacing compared to cases with $\lambda/2$ and $\lambda/3$ grids. Note that the curve of $R2 = 0.65R1$ has a good linearity while offering a phase variation about $280°$.

The reflected phase curves with different ring spacings at 10 GHz in a $\lambda/5$ grid are illustrated in Fig. 5. It is apparently seen that the ring spacing has nearly no effects on the linearity of the reflected phase curves as well as the reflected phase range. That indicates the ring spacing becomes irrelevant when the sub-wavelength grids shrink to a certain size. It is observed in Fig. 5 that all curves exhibit a relatively good linearity while providing a phase range about $250°$.

2.2. Bandwidth Performance on Various Grid Spacings

Figure 6 plots the reflected phasing curves of the double concentric circular ring element with various grid spacings for different frequencies. The ring spacings of $R2 = 0.8R1$, $R2 = 0.5R1$, $R2 = 0.65R1$ and $R2 = 0.8R1$ are chosen to achieve relatively good linearity and reflected phase range for the $\lambda/2$, $\lambda/3$, $\lambda/4$ and $\lambda/5$ grids, respectively. It is noticed in Fig. 6 that the phase curves feature more linear
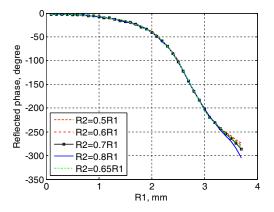
Figure 4. Reflected phase curves with different ring spacings at $10\,\text{GHz}$ in a $\lambda/4$ grid.
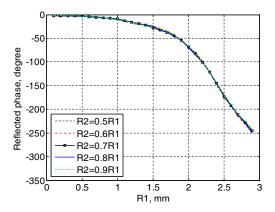
Figure 5. Reflected phase curves with different ring spacings at $10\,\text{GHz}$ in a $\lambda/5$ grid.
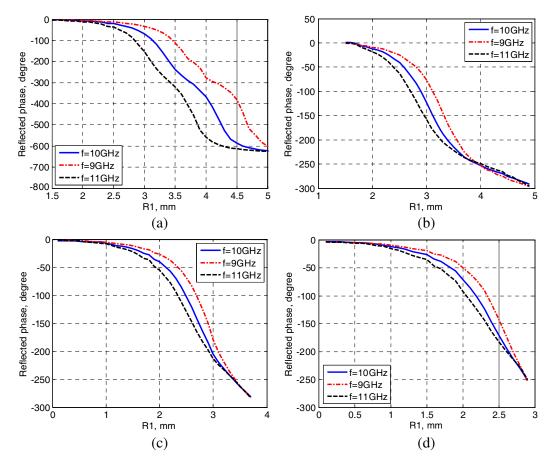

Figure 6. Reflected phase curves of the double concentric circular ring element with various grids for different frequencies. (a) $\lambda/2$ grid with ring spacing of $R2 = 0.8R1$, (b) $\lambda/3$ grid with ring spacing of $R2 = 0.5R1$, (c) $\lambda/4$ grid with ring spacing of $R2 = 0.65R1$ and (d) $\lambda/5$ grid with ring spacing of $R2=0.8R1$.

behaviour and less sensitive to the frequency variation with the decrease of the grid size. Therefore, a broadband performance is expected to be obtained with sub-wavelength grids. However, the reflected phase range is also reduced with smaller grid spacing. The reduced span of phase increases phase errors and result in poorer collimation of energy in the reflectarray's main beam. This will be investigated more in detail in the later section.

2.3. Magnitude of Reflected Energy of Unit Cell with Various Grid Spacings

In addition to the reflected phase, the magnitude of the reflected energy of the double concentric circular ring element in a unit cell environment is also studied. Fig. 7 shows the magnitude of the reflected energy of the double concentric circular ring element with various grid spacings at 10 GHz. Theoretically, since all metallic surfaces are modelled as PEC in simulations, the losses are attributed to the loss tangent of the RO4003 substrate. The polycarbonate layer is considered lossless. While the losses in all four grid spacings are generally low which indicates a good efficiency, the trend of loss reduction through decreasing the grid sizes is evident. As can be seen in Fig. 7, for the case of $\lambda/2$ grid, the maximum reflection loss is less than 0.35 dB while for the case of $\lambda/5$ grid, the maximum reflection loss is less than only 0.06 dB.
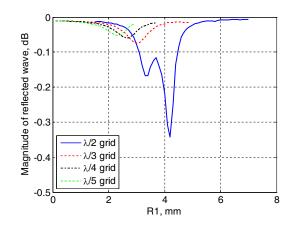

Figure 7. Reflected magnitude curves of the double concentric circular ring element with different grid spacings at 10 GHz.

The results provide a clue to why a sub-wavelength spacing has wider bandwidth compared to the conventional $\lambda/2$ spacing. At the resonance, energy from the incident plane wave excites the double ring element. Around the resonant frequency, energy is trapped and dissipated in accordance with the loss tangent of the substrate. At the resonant frequency, the elements radiate efficiently and one obtains a good efficiency. However, as one moves away from the resonant frequency, the efficiency drops off quickly.

On the other hand, the double ring element in sub-wavelength grid spacing is not resonant and most of the incident energy is reflected with a phase variation commensurate with the parameters of the double ring element. In fact, this is what one desires in an element for reflectarray — as much energy reflected as possible. As the element is not resonant, the variation with regards to frequency is less significant. Therefore, the bandwidth of a sub-wavelength grid spacing is expected to be wider.

3. IMPLEMENTATION AND PERFORMANCE OF THE REFLECTARRAYS

3.1. Feed Horn Design and Performance

In this work, a pyramidal horn antenna is designed and manufactured to illuminate the reflectarray. The critical parameters of the pyramidal horn are optimised by HFSS to achieve the desired behaviour at the operational band. Fig. 8 illustrates the pyramidal horn antenna prototype. The return loss was tested by using an Agilent N5244A network analyser and the radiation patterns were measured inside an anechoic chamber.

The simulated and measured return losses of the pyramidal horn are shown in Fig. 9. It is evident that the measured result agrees well with the simulated one and the proposed horn exhibits a 10-dB return loss bandwidth from 7.85 GHz to 12.6 GHz, which covers the interesting band.

Figure 10 plots the radiation patterns of the proposed pyramidal horn at 10 GHz. It is observed in Fig. 10 that both principal planes feature a peak gain of 13 dBi with a 10-dB beamwidth of 76°, which

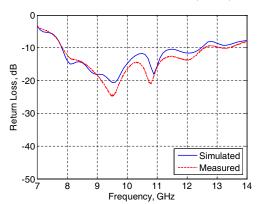**Figure 8.** Prototype of the feed pyramidal horn antenna.

Figure 9. Simulated and measured return loss curves of the feed pyramidal horn antenna.
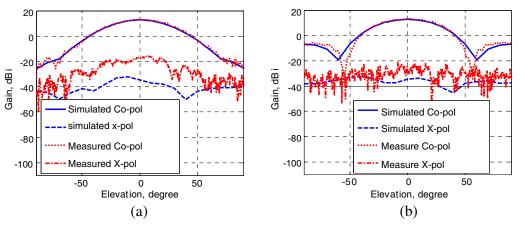

Figure 10. Simulated and measured radiation patterns of the feed pyramidal horn antenna at 10 GHz. (a) E-plane and (b) H-plane.

is good for a proper illumination on reflectarrays. In addition, a low cross-polarisation performance is also obtained.

3.2. Reflectarray Realization and Performance

In this study, a 10-dB edge illumination of the reflectarray is assumed. An offset feed method ($\theta_i = 25°$) is adopted to avoid aperture blockage and the elements' reflection phases are adjusted to generate a main beam 25° off broadside. Four X-band reflectarrays with $\lambda/2$, $\lambda/3$, $\lambda/4$ and $\lambda/5$ grid spacings are designed and fabricated, all at 10 GHz. Every antenna has a square aperture of 430 mm × 430 mm hosting 729, 1640, 2809 and 4623 elements for $\lambda/2$, $\lambda/3$, $\lambda/4$ and $\lambda/5$ arrays, respectively. Prototypes of the reflectarrays are shown in Fig. 11.

Figure 12 presents the measured radiation patterns of four reflectarrays at 10 GHz. It is seen that the main beams occur at 25° off-broadside in all four reflectarrays. The measured side lobe levels are better than 15 dB in both principal planes except the $\lambda/5$ array where the side lobe level is better than 13 dB. It is also observed that at the region around the main lobe, the cross polarisation levels are about 25 dB in both planes.

The measured Gain versus Frequency of the reflectarrays is compared in Fig. 13. The antenna gains were measured over the frequency range from 8.2 GHz to 12.4 GHz. The measured maximum gains are 29.2 dBi, 29.2 dBi, 28.6 dBi and 25.8 dBi for $\lambda/2$, $\lambda/3$, $\lambda/4$ and $\lambda/5$ arrays, respectively. Using a 2-dB gain bandwidth as a criterion, one notes that the $\lambda/4$ array is able to achieve a 33% bandwidth compared to a 15% bandwidth of the $\lambda/2$ array. However, the $\lambda/4$ array's peak gain is slightly lower at 28.6 dBi compared to 29.2 dBi of the $\lambda/2$ array. The $\lambda/5$ array also demonstrates similar bandwidth but the peak gain is significantly lower at 25.8 dBi.
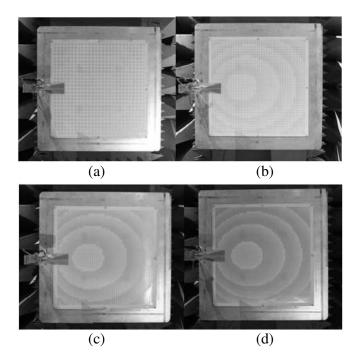
Figure 11. Prototypes of the reflectarrays. (a) $\lambda/2$ array with 729 double concentric circular rings, (b) $\lambda/3$ array with 1640 double concentric circular rings, (c) $\lambda/4$ array with 2809 double concentric circular rings and (d) $\lambda/5$ array with 4623 double concentric circular rings.
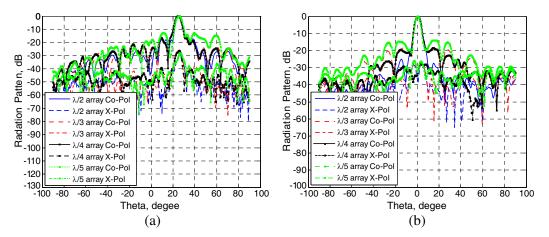

Figure 12. Measured radiation patterns in principal planes at 10 GHz for four reflectarrays. (a) x-z plane and (b) on the plane forming an angle of 25 degrees with y-z plane.

3.3. Discussion

Table 1 summarizes the performances of four reflectarrays. The reference is the conventional reflectarray with a grid spacing of $\lambda/2$. In general, the peak gain of reflectarrays drops when the grid spacing gets smaller. The exception is for the case of $\lambda/3$ array where its maximum gain still remains as the same 29.2 dBi as that obtained in the $\lambda/2$ array. This is obtained despite the phase range of the element in a unit cell is reduced significantly to 290°. For the $\lambda/4$ array, the reflected phase range of 280° in the unit cell results in a 0.6 dB loss in antenna gain relative to the $\lambda/2$ and $\lambda/3$ arrays. This 0.6 dB loss is a design compromise since it exhibits a remarkably wider gain bandwidth of 33% compared to 15% and 21% of $\lambda/2$ and $\lambda/3$ arrays, respectively. This significant bandwidth enhancement is due to the phase curves in the unit cell for $\lambda/4$ array showing more linear and similar behaviour over a wider frequency range
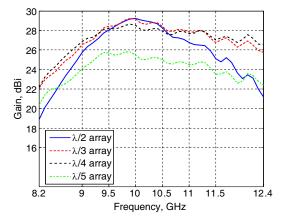
Figure 13. Measured gain of the reflectarrays.

Table 1. Performances of four reflectarrays.

	$\lambda/2$ array	$\lambda/3$ array	$\lambda/4$ array	$\lambda/5$ array
Maximum Gain (dBi)	29.2	29.2	28.6	25.8
2-dB Gain Bandwidth (%)	15	21	33	24
2-dB Gain Bandwidth (GHz)	9.3–10.8	9.3–11.4	9–12.3	9–11.4
Peak Aperture Efficiency (%)	40.1	40.1	36.2	18.1
Unit Cell Reflected Phase Range	$\sim 640°$	$\sim 290°$	$\sim 280°$	$\sim 250°$

compared to the ones for $\lambda/2$ and $\lambda/3$ arrays, therefore resulting in a relatively broadest bandwidth. As for the $\lambda/5$ array, although the gain bandwidth of 24% is still reasonably wide, its maximum gain of 25.8 dBi is significantly lower compared to other three reflectarrays, and subsequently very poor aperture efficiency. This is due to the unit cell's reflected phase range of only 250°. For a moderately sized reflectarray of about $14.5\lambda \times 14.5\lambda$ as in this case, it is surmised that the unit cell's reflected phase range of about 300° is necessary to design a reflectarray with about 30% bandwidth. In summary, there is a compromise between the reflectarray gain and bandwidth when the single-layered double concentric ring elements are applied on sub-wavelength grids.

4. CONCLUSION

The concept of using single-layer double concentric circular ring elements on various sub-wavelength grids for reflectarray bandwidth improvement has been studied both numerically and experimentally. Numerical investigations are conducted to understand the broadband mechanism of single-layer sub-wavelength multi-resonant elements. As an alternative to the traditional sub-wavelength single patch designs that have only one variable parameter of the phasing element, additional parameters of the double concentric circular ring element such as the spacing between the two rings are varied to achieve a good performance when applied on various sub-wavelength grids. In addition, the trade-off between the reflectarray gain and bandwidth needs to be addressed when using single-layered double concentric ring elements on sub-wavelength grids. The measured results show the $\lambda/4$ array achieves a considerable bandwidth improvement compared to the $\lambda/2$ array, where the 2-dB gain bandwidth has been increased from 15% to 33%.

REFERENCES

1. Huang, J. and J. A. Encinar, "Reflectarray antennas," John Wiley & Sons, Institute of Electrical and Electronics Engineers, 2008.

2. Li, Q. Y., Y. C. Jiao, and G. Zhao, "A novel microstrip rectangular-patch/ring combination reflectarray element and its application," *IEEE Antennas Wireless Propag. Lett.*, Vol. 8, 1119–1122, 2009.

3. Li, R. H., L. Chen, X. T. Gu, and X. W. Shi, "A novel element for broadband reflectarray antennas," *Journal of Electromagnetic Waves and Applications*, Vol. 25, Nos. 11–12, 1554–1563, 2011.

4. Encinar, J. A. and J. A. Zomaza, "Broadband design of three-layer printed reflectarrays," *IEEE Transactions on Antennas and Propagation*, Vol. 51, No. 7, 1662–1664, Jul. 2003.

5. Encinar, J. A., "Design of two-layer printed reflectarrays using patches of variable size," *IEEE Transactions on Antennas and Propagation*, Vol. 49, No. 10, 1403–1410, Oct. 2001.

6. Li, Y., M. E. Biakowski, K. H. Sayidmarie, and N. V. Shuley, "81-element single-layer reflectarray with double-ring phasing elements for wideband applications," *2010 IEEE Antennas and Propagation Society International Symposium*, 1–4, Toronto, Canada, Jul. 11–17, 2010.

7. Li, Y., M. E. Biakowski, K. H. Sayidmarie, and N. V. Shuley, "Single-layer microstrip reflectarray with double elliptical ring elements for bandwidth enhancement," *Microwave and Optical Technology Letters*, Vol. 53, No. 5, 1083–1087, May 2011.

8. Robinson, A. W., M. E. Bialkowski, and H. J. Song, "A passive reflect-array with duaal-feed microstrip patch elements," *Microwave and Optical Technology Letters*, Vol. 23, No. 5, 295–299, Dec. 5, 1999.

9. Robinson, A. W., M. E. Bialkowski, and H. J. Song, "An 137-element active reflect-array with dual-feed microstrip patch elements," *Microwave and Optical Technology Letters*, Vol. 26, No. 3, 147–151, Aug. 2000.

10. Pozar, D. M., "Wideband reflectarrays using artificial impedance surfaces," *Electron. Lett.*, Vol. 43, No. 3, 148–149, Feb. 2007.

11. Nayeri, P., F. Yang, and A. Z. Elsherbeni, "Bandwidth improvement of reflectarray antennas using closely spaced elements," *Progress In Electromagnetics Research C*, Vol. 18, 19–29, 2011.

12. Nayeri, P., F. Yang, and A. Z. Elsherbeni, "Broadband reflectarray antennas using double-layer sub-wavelength patch elements," *IEEE Antennas Wireless Propag. Lett.*, Vol. 9, 1139–1142, 2010.

13. Bialkowski, M. and K. H. Sayidmarie, "Investigations into phase characteristics of a single-layer reflectarray employing patch or ring elements of variable size," *IEEE Transactions on Antennas and Propagation*, Vol. 56, No. 11, 3366–3372, Nov. 2008.

14. Bialkowski, M. and K. H. Sayidmarie, "Phasing characteristics of variable size double rings of square or circular shape for design of a single layer microstrip reflectarray," *17th International Conference on Microwave, Radar and Wireless Communications*, 1–4, Wroclaw, Poland, May 19–21, 2008.

15. Sayidmarie, K. H. and M. Bialkowski, "Investigations into unit cells offering an increased phasing range for single-layer printed reflectarrays," *Microwave and Optical Technology Letters*, Vol. 50, No. 4, 1028–1032, Apr. 2008.

16. Targonski, S. D. and D. M. Pozar, "Analysis and design of a microstrip reflectarray using patches of variable size," *Antennas Propag. Soc. Int. Symp. Dig.*, 1820–1823, Seattle, WA, Jun. 20–24, 1994.